Acta Crystallographica Section C
Crystal Structure Communications
ISSN 0108-2701

Hexagonal high-temperature form of aluminium phosphate tridymite from X-ray powder data

Heribert A. Graetsch

Institut für Geologie, Mineralogie und Geophysik, Ruhr-Universität Bochum, D-44780 Bochum, Germany
Correspondence e-mail: heribert.graetsch@ruhr-uni-bochum.de

Received 26 January 2001
Accepted 22 March 2001

Similar to silica tridymite, $AlPO_4$ tridymite shows a sequence of displacive phase transitions resulting in a dynamically disordered hexagonal high-temperature modification. Rietveld refinement reveals that the thermal motions of the tetrahedra can be described either by strongly anisotropic displacement parameters for oxygen or by split O atoms. Due to the ordered distribution of aluminium and phosphorus over alternating tetrahedra, the space group symmetry of high-temperature $AlPO_4$ tridymite is reduced with respect to SiO_2 tridymite from $P6_3/mmc$ to $P6_3mc$.

Comment

$AlPO_4$ crystallizes in several modifications which are isotypic with the silica minerals quartz, tridymite and cristobalite (Flörke, 1965). The latter two are high-temperature forms which persist metastably at ambient conditions. $AlPO_4$ and SiO_2 tridymites show a similar sequence of displacive phase transitions upon heating and several forms with different superstructures at room temperature (Spiegel *et al.*, 1990). The transition temperatures are shifted to lower values for $AlPO_4$ tridymite. Whereas the crystal structures of most of the silica tridymite phases are known, only two room-temperature forms of $AlPO_4$ tridymite have been refined so far (Graetsch, 2000). The present refinement of the hexagonal high-temperature modification of $AlPO_4$ tridymite was carried out in the course of an investigation of the phase transitions of tridymite. Due to the lack of suitable single crystals, a powder sample was used. The framework structure of tridymite consists of corner-sharing tetrahedra which form layers made up by six-membered rings of tetrahedra. Antiparallel layers are stacked in the direction of the hexagonal *c* axis, forming a two layer sequence. Viewed along the *c* axis, the vertices of the tetrahedra alternatively point up and down (Fig. 1*a*). All tetrahedra have the same size in silica tridymite, whereas tetrahedra occupied either by aluminium or phosphorus have different sizes in $AlPO_4$ tridymite. The cation distribution is ordered as in all other $AlPO_4$ polymorphs so that all up-pointing tetrahedra are exclusively occupied by either aluminium or phosphorus (depending on the point of view). This destroys the mirror plane perpendicular to the 6_3 screw axis and reduces the symmetry from $P6_3/mmc$ (No. 194) for hexagonal SiO_2 tridymite to $P6_3mc$ (No. 186) for $AlPO_4$ tridymite. The structure of hexagonal $AlPO_4$ high tridymite is dynamically disordered, as can be seen by the large and strongly anisotropic displacement parameters of the O atoms which are small along directions connecting Al and P atoms and large in perpendicular or inclined directions (Fig. 1*b*), whereas the displacement ellipsoids of the cations are almost spherical. This indicates that the thermal motions are most likely dominated by so-called rigid-unit modes which leave the stiff tetrahedra almost undistorted (*cf.* Pryde & Dove, 1998). The average structure with all atoms on special positions yields an idealized picture; the shape of the tetrahedra rings is perfectly hexagonal, the Al—O and P—O bonds being 1.66 (1) and 1.46 (1) Å, respectively, and the corresponding O–O edges of the tetrahedra [2.72 (1) and 2.38 (1) Å] are shorter than the room-temperature values. The inter-tetrahedral Al—O—P angles are linear (180°) instead of approximately 147°, as has been found for the room-temperature forms (Graetsch, 2000).

More realistic interatomic distances and angles can be obtained by using a split-atom model for the O atoms in order to describe the dynamic disorder that has been shown by

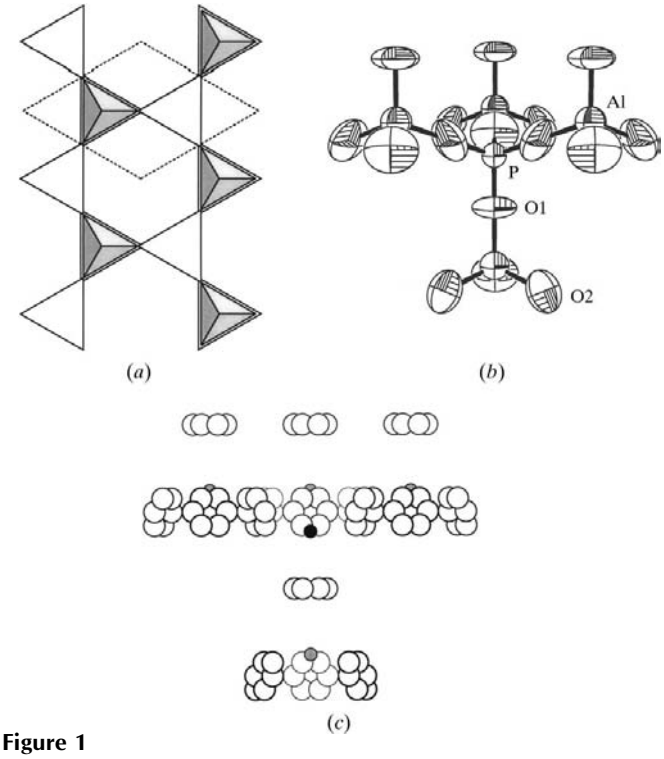

Figure 1
(*a*) Polyhedral representation of hexagonal high-temperature $AlPO_4$ viewed along the *c* axis (the AlO_4 tetrahedra are white and the PO_4 tetrahedra are shaded), (*b*) *ORTEP*-3 (Farrugia, 1997) plot of the average structure with 50% probability displacement ellipsoids, and (*c*) representation of the split-atom model perpendicular to the *c* axis.

 © 2001 International Union of Crystallography • Printed in Great Britain – all rights reserved

Kihara (1980) for high-temperature silica tridymite and by Peacor (1973) and Wright & Leadbetter (1975) for β-cristobalite. For a split-atom model of $AlPO_4$ tridymite, the two symmetrically non-equivalent O atoms of the average structure were removed from the 2*b* and 6*c* positions and distributed over four general 12*d* positions of space group $P6_3mc$ with occupancy $\frac{1}{6}$, so that they are located on circles between the Al and P atoms (Fig. 1*c*). Rietveld refinement showed that the split-atom model with one overall isotropic displacement parameter describes the diffraction pattern equally well, but the Al—O and P—O distances remain close to the values of 1.72 (1) and 1.51 (1) Å, respectively, found by Muraoka & Kihara (1997) for the quartz form of $AlPO_4$ (berlinite) at room temperature. The average inter-tetrahedral Al—O—P angle is 150° and the radius of the circles populated by six equidistant split O atoms refined to *ca* 0.4 Å, which is much the same as for high-temperature silica cristobalite and tridymite (Peacor, 1973; Wright & Leadbetter, 1975; Kihara, 1980).

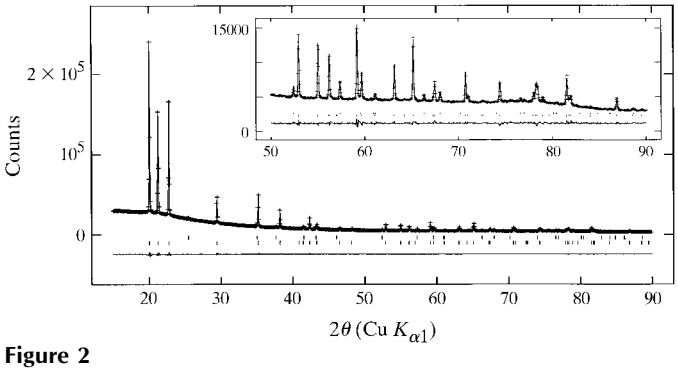

Figure 2
Comparison of the observed (crosses) and calculated (solid line) powder-diffraction patterns of high-temperature $AlPO_4$ tridymite (average structure) and corundum (*ca* 4 wt%) at *ca* 593 K. The difference pattern is shown below. The short bars indicate the positions of the reflections.

The average structure and split-atom model refined to the same *wRp* values for the same number of variables so that it was not possible to gain further insight into the nature of the disorder from X-ray powder refinements, *i.e.* to distinguish between free vibrations of the tetrahedra or dynamic microtwins.

Experimental

$AlPO_4$ tridymite was prepared by annealing non-crystalline $AlPO_4$ (Merck No. 1.01098.1000) at 1223 K for 1 d. The sample consisted of 87 wt% triclinic, 9 wt% monoclinic tridymite and 4 wt% corundum at room temperature (*cf.* Graetsch, 2000). The latter was utilized as an additional internal standard for the temperature control. Above 373 K, only a single incommensurate high-temperature tridymite phase showed up in the X-ray powder diagrams together with corundum. Near 573 K, a gradual transition to hexagonal high-temperature $AlPO_4$ took place. The diffractogram used for Rietveld refinements was recorded at *ca* 593 (15) K in transmission mode using a focusing Ge(111) monochromator.

Average structure

Crystal data

$AlPO_4$
M_r = 121.95
Hexagonal, $P6_3mc$
a = 5.0976 (3) Å
c = 8.3441 (4) Å
V = 187.77 (2) Å^3
Z = 2
D_x = 2.157 (1) Mg m^{-3}
Cu $K\alpha_1$ radiation
μ = 8.0 mm^{-1}
T = 593 K
Specimen shape: cylinder
10.0 × 0.5 × 0.5 mm
Specimen prepared at 1223 K
Particle morphology: plate-like
White powder

Data collection

Siemens D5000 diffractometer
Specimen mounting: 0.5 mm glass capillary
Specimen mounted in transmission mode
T = 593 K
$2\theta_{min}$ = 15, $2\theta_{max}$ = 90°
Increment in 2θ = 0.008°

Refinement

Refinement on I_{net}
R_p = 0.013
R_{wp} = 0.019
R_{exp} = 0.010
S = 1.95
Wavelength of incident radiation: 1.540562 Å
Excluded region(s): none
Profile function: pseudo-Voigt
41 parameters
$(\Delta/\sigma)_{max}$ = 0.01
Preferred orientation correction: none

Split-atom model

Crystal data

$AlPO_4$
M_r = 121.95
Hexagonal, $P6_3mc$
a = 5.0976 (3) Å
c = 8.3441 (4) Å
V = 187.77 (2) Å^3
Z = 2
D_x = 2.157 Mg m^{-3}
Cu $K\alpha_1$ radiation
μ = 8.0 mm^{-1}
T = 593 K
Specimen shape: cylinder
10.0 × 0.5 × 0.5 mm
Specimen prepared at 1223 K
Particle morphology: plate-like
White powder

Data collection

Siemens D5000 diffractometer
Specimen mounting: 0.5 mm glass capillary
Specimen mounted in transmission mode
T = 593 K
$2\theta_{min}$ = 15, $2\theta_{max}$ = 90°
Increment in 2θ = 0.008°

Refinement

R_p = 0.013
R_{wp} = 0.019
R_{exp} = 0.010
S = 2.15
Wavelength of incident radiation: 1.540562 Å
Excluded region(s): none
Profile function: pseudo-Voigt
41 parameters
$(\Delta/\sigma)_{max}$ = 0.01
Preferred orientation correction: none

The crystal structure was refined according to the Rietveld method (Rietveld, 1969) using the *GSAS* program package (Larson & von Dreele, 1994). Initially, lattice parameters, six peak-shape parameters of the pseudo-Voigt function (No. 2), one asymmetry parameter and one parameter for the zero-point correction were refined without a structure model according to the LeBail method (LeBail *et al.*, 1988). The high background at low 2θ caused by the position-sensitive detector was removed by the fixed background subtraction feature of the *GSAS* program package. Remaining background was fitted with six parameters using a power series function (No. 6). The structure refinement was started with the atomic coordinates of the isotypic hexagonal high-temperature silica tridymite phase at 733 K (Kihara, 1978). Unlike $AlPO_4$ cristobalite and berlinite, no extra reflections were found for hexagonal $AlPO_4$ tridymite with respect to its silica analog. Extinctions indicate as possible space groups $P6_3/mmc$,

$P6_3mc$, $P6\bar{2}c$, $P\bar{3}c1$ and $P31c$, however, a framework of alternating AlO_4 and PO_4 tetrahedra is only compatible with $P6_3mc$ and $P31c$. Refinements in space group $P31c$ yielded no lower R values than in $P6_3mc$, in spite of an additional refinable positional parameter for O2. The z positional parameter of the Al atom was fixed in order to define the origin in space group $P6_3mc$. Soft constraints were set on the interatomic distances so that the sizes of the tetrahedra should remain close to those of $AlPO_4$ quartz: Al—O = 1.73, O—O = 2.83, P—O = 1.52 and O—O = 2.49 Å (Muraoka & Kihara, 1997), but refined to 1.66, 2.72, 1.45 and 2.38 Å, respectively, for the average structure. The change from individual isotropic to anisotropic displacement parameters reduced the *wRp* value from 0.027 to 0.019 (for 34 and 41 variables, respectively) and $R(F^2)$ from 0.088 to 0.045 (for 70 reflections). Refinement of the split-atom model for the O atoms did not result in lower R values but in more realistic interatomic distances which are close to those of berlinite. Corrections for absorption and extinction were found to be unnecessary. Preferred orientation was not observed. The small step size of 0.008° 2θ most likely leads to artificially low standard deviations (*cf*. Hill & Flack, 1987; Baerlocher & McCusker, 1994). In order to obtain correct values, only every seventh data point was used in a final refinement cycle with fixed profile parameters. The Durban–Watson d statistic value became close to 2 (1.98). This procedure increased the s.u.'s by a factor of approximately four with respect to those obtained with the original data set.

For both compounds, data collection: *DIFFRAC-AT* (Version 3.0; Siemens, unpublished); cell refinement: *GSAS* (Larson & von Dreele, 1994); data reduction: *GSAS*; program(s) used to solve structure: *GSAS*; program(s) used to refine structure: *GSAS*; molecular graphics: *ORTEP*-3 (Farrugia, 1997) for the average structure and *WATOMS* (Dowty, 1994) for the split-atom model; software used to prepare material for publication: *WINWORD*97.

Supplementary data for this paper are available from the IUCr electronic archives (Reference: BR1322). Services for accessing these data are described at the back of the journal.

References

Baerlocher, C. & McCusker, L. B. (1994). *Advanced Zeolite Science and Applications*, ch. 13, pp. 391–428. Amsterdam: Elsevier.
Dowty, E. (1994). *WATOMS*. Shape Software, 521 Hidden Valley Road, Kingsport, Tennessee, USA.
Farrugia, L. J. (1997). *J. Appl. Cryst.* **30**, 565.
Flörke, O. W. (1965). *Sci. Ceram.* **3**, 13–27.
Graetsch, H. (2000). *Acta Cryst.* C**56**, 401–403.
Hill, R. J. & Flack, H. D. (1987). *J. Appl. Cryst.* **20**, 356–361.
Kihara, K. (1978). *Z. Kristallogr.* **148**, 237–253.
Kihara, K. (1980). *Z. Kristallogr.* **152**, 95–101.
Larson, A. C. & von Dreele, R. B. (1994). *LANSCE* (MS-H805), Los Alamos National Laboratory Report LAUR 86–748. Los Alamos, New Mexico, USA.
LeBail, A., Duroy, H. & Fourquet, J. L. (1988). *Mater. Res. Bull.* **23**, 447–452.
Muraoka, Y. & Kihara, K. (1997). *Phys. Chem. Miner.* **24**, 243–253.
Peacor, D. R. (1973). *Z. Kristallogr.* **138**, 274–298.
Pryde, A. K. A. & Dove, M. T. (1998). *Phys. Chem. Miner.* **26**, 171–179.
Rietveld, H. M. (1969). *J. Appl. Cryst.* **2**, 65–71.
Spiegel, M., Hoffmann, W. & Löns, J. (1990). *Eur. J. Miner.* **2**, 246.
Wright, A. F. & Leadbetter, A. J. (1975). *Philos. Mag.* A**31**, 1391–1401.